IEEE Access
Multidisciplinary | Rapid Review | Open Access Journal

Received March 11, 2020, accepted March 24, 2020, date of publication April 2, 2020, date of current version April 20, 2020.

Digital Object Identifier 10.1109/ACCESS.2020.2985051

Variable Scale Relative Entropy Detection for Non-Cooperative Underwater Acoustic Pulse Signals

KUN WEI, SHILIANG FANG, AND JUN TAO (Member, IEEE)
Key Laboratory of Underwater Acoustic Signal Processing of Ministry of Education, Southeast University, Nanjing 210096, China
Corresponding authors: Kun Wei (wkchase@seu.edu.cn) and Shiliang Fang (slfang@seu.edu.cn)

This work was supported in part by the National Natural Science Funds of China under Grant 61871114, Grant 11574048, Grant 11674057, Grant 11604048, Grant 11704069, and Grant 11874109, and in part by the Fundamental Research Funds for the Central Universities under Grant 2242020k30044.

ABSTRACT This work investigates the detection of non-cooperative underwater acoustic pulse signals at low signal-to-noise ratio (SNR). A variable scale relative entropy (VSRE) pulse signal detection scheme is proposed. Different from conventional relative entropy (RE) method where an observation sequence is processed at a given scale for detection, the proposed scheme performs the processing at multiple different scales. As a result, the original RE difference vector becomes a RE difference matrix, each column corresponding to a particular scale. Before a decision is made, the VSRE difference matrix is post-processed for improved fidelity. The non-zero elements of the resulting VSRE difference matrix are divided into groups, each corresponding to a pulse signal, based on their occurrence times within the observation sequence. Within each group, the one with the maximum RE difference is chosen to determine the exact appearance time and duration of the pulse signal. The performance gain of the VSRE detector over existing RE detector has been verified by both simulation and at-sea experimental results.

INDEX TERMS Non-cooperative detection, underwater acoustic pulse signals, variable scale relative entropy.

I. INTRODUCTION

A non-cooperative underwater acoustic pulse signal may come from a mechanical collision, an underwater explosion, an active sonar of the other side, and so on. Its time duration (width) can vary from a few milliseconds to a few seconds. Detection of a non-cooperative underwater acoustic pulse signal is of great significance in practical applications such as target recognition, early warning, and so on. Non-cooperative underwater acoustic pulse signal detection systems aim to find a target pulse without priori information such as the time of occurrence, width, center frequency, amplitude, etc [1], [2]. Due to the lack of prior knowledge, the task of non-cooperative detection is very challenging.

Conventional non-cooperative detection methods include the energy-based detection method [3], the entropy-based detection method [5], and the time-frequency analysis methods [6]–[9]. In [3], an energy-based detection method is proposed. It includes two steps: first, the signal energy and background noise energy are estimated by the rainbow click algorithm [4]; second, a non-parametric page test (NPT) is performed with the energy difference. The performance of the detection scheme is evaluated via simulations for different types of pulse signals. It showed the performance degrades rapidly as the signal-to-noise ratio (SNR) decreases. An entropy-based detection method outperforms an energy-based method at low SNRs by making use of the difference in statistical characteristic between a signal and a noise. In [5], two entropy-based detection methods are proposed for intercept processing of the sonar signals: the Fourier transform (FT) based entropy method and the wavelet transform (WT) based entropy method, both having low complexity good for real-time applications. They are tested by three pulse signals including the frequency-hopped (FH) pulse, the broadband communication pulse, and the low probability of intercept (LPI) pulse. It shows the FT-based method works better for the FH and broadband communication pulses while the WT-based method excels for the LPI pulse.

The associate editor coordinating the review of this manuscript and approving it for publication was Emrecan Demirors.

The time-frequency analysis methods make detections by utilizing both time-domain and frequency-domain characteristics of signals. They are categorized into four types: the short-time Fourier transform (STFT) method, the Wavelet Transform (WT) method, the Wigner-Ville distribution (WVD) method, and the fractional Fourier transform (FrFT) method. In [6], Hlawatsch and Bartels gave a tutorial review of the STFT method. It is easy to implement but cannot achieve high resolutions in the time domain and frequency domain simultaneously. In [7], David and Chapron proposed a WT method. It achieves a more flexible time-frequency analysis than the STFT. However, aliasing and energy leakage happen due to its poor band isolation. In [8], detection techniques based on the WVD and cross-WVD (XWVD) are proposed and tested by real data. Good noise rejection performance are obtained. Even though, they suffer the problem of cross-term interference which affects its practicability. The FrFT-based detection [9] is advantageous for detecting LFM signal, but its performance is sensitive to the multipath. In [10], Zhang proposed to combine the time-reversal focusing with the FrFT method, leading to improved performance.

In addition to the aforementioned classical detection algorithms, some emerging methods have also been proposed recently. Kumar *et al.* proposed an intercept detection method for low-SNR targets [11]. It employs a new beamforming scheme and a dynamic threshold to achieve a constant false alarm rate, irrespective of the intercepted frequency. Even though, the detection performance under non-stationary noise environments cannot be guaranteed. In [12], a non-cooperative method based on the two-sample Kolmogorov-Smirnov (K-S) test was proposed to achieve blind signal detection in symmetric alpha-stable noise. Empirical cumulative distribution functions (ECDFs) of the received signal and the noise are required. Simulation results showed the K-S detector is effective only in symmetric alpha-stable noise though. In [13], a detection algorithm based on the stochastic resonance (SR) was designed for detecting underwater acoustic weak signal. It, however, is unstable without prior information. Motivated by the success of relative entropy (RE) method in multi-input multi-output (MIMO) radar [14], [15], Mignerey studied the feasibility of an RE based distributed passive detection scheme [16]. It is found the resulting RE detector is insensitive to statistical dependence among the sensors and achieves good performance despite of pulse type. Due to its superiority, the RE has also found wide application in other fields than the underwater pulse detection [17], [18].

The RE method is robust under non-stationary ocean environments. However, it does not achieve satisfactory performance for combined pulses with different pulse widths and/or under low SNR conditions. This motivates the recent investigation on a variable scale relative entropy (VSRE) based detection [19]. Preliminary simulation results showed its superiority over the conventional RE detection while experimental verification is lacking. In the current paper, a postprocessing procedure is introduced to the VSRE detector, leading to a much improved scheme for adaptive search of pulses. The resulting improved VSRE detector is able to distinguish multiple pulses of different types and widths within a given observation sequence. A candidate set of scales are determined based on the size of the observation sequence and a preset minimum pulse width. For a given scale, a RE difference vector is computed as in a conventional RE detector. The RE difference vectors of all scales are combined into a RE difference matrix, which is further processed such that only entries corresponding to potential signal pulses are kept untouched and others are set to zeros. Such a postprocessing procedure leads to extra performance gain over [19]. To make a detection based on the postprocessed RE difference matrix, its nonzero elements are divided into groups, according to their row and column indices. Each group corresponds to a target pulse, with its exact starting time and width determined by the row/column information of the largest element within the group. Extensive simulation and experiment results are provided to demonstrate the superior performance of the VSRE detector.

The rest of this paper is organized as follows. Section II reviews the basic theory of the relative entropy detection, in particular the kernel density estimation (KDE). The VSRE detector is discussed in Section III. Simulation and experimental results are presented in Section IV and Section V, respectively. Finally, Section VI concludes the paper.

Notation: For a random variable X, its probability density function (PDF) is given as $f(x)$. The $(\cdot)^T$ denotes the matrix transpose, and $\|\cdot\|$ is the Euclidean norm.

II. PRELIMINARIES

For a binary hypothesis testing problem, the task is to decide whether a given observation sequence is pure noise (null hypothesis $\mathcal{H}_0$) or signal plus noise (alternative hypothesis $\mathcal{H}_1$) [20]. It is assumed the observation sequence contains independent and identically distributed (i.i.d) samples that follow $X \sim f(x)$. In the non-cooperative scenario, the goal is achieved by deciding whether the observation sequence has a similar statistical characteristic to an i.i.d probe (ambient noise) sequence, $X_p \sim f_p(x)$. To measure the statistical difference between X and X_p, the RE has been proposed as a measurement metric [16]. The definition of RE between two PDFs, $f_p(x)$ and $f(x)$, is [21]–[23]

$$D_{p,f} = D\left[f_p(x)||f(x)\right] = \mathbb{E}_p\left[\log\left(\frac{f_p(x)}{f(x)}\right)\right] \tag{1}$$

which is also called the Kullback-Leibler (KL) divergence [23, Ch. 1.3]. In (1), the expectation is with respect to $f_p(x)$. When the observed contains mainly ambient noise, we expect $D_{p,f}$ to be small or close to zero. Otherwise, the observed can be a pulse signal plus noise.

To make a decision, one still needs a detection threshold (DT). It can be obtained by measuring the RE between the probe sequence and another non-overlapping i.i.d ambient noise sequence with a distribution $X_q \sim f_q(x)$, that is $\gamma = D\left[f_p(x)\,||\,f_q(x)\right]$. It is noted for passive surveillance

systems, noises are observed most of time and it is not difficult to get two non-overlapping ambient noise sequences. The RE detector then makes a decision as follows

$$D_{p,f} \underset{\mathcal{H}_0}{\overset{\mathcal{H}_1}{\gtrless}} \gamma \tag{2}$$

or equivalently

$$D_{p,f} - \gamma \underset{\mathcal{H}_0}{\overset{\mathcal{H}_1}{\gtrless}} 0 \tag{3}$$

In practice, however, the PDFs of the probe and observation sequences are unknown thus have to be estimated. The kernel density estimation (KDE) method is classical algorithm to estimate the PDF of a random variable. Based on the observation samples $[x_1\ x_2 \cdots x_N]^T$, the KDE gives the following PDF estimation

$$\hat{f}(x) = \frac{1}{N}\sum_{n=1}^{N}\phi(x, x_n; b), \quad x \in \mathbb{R} \tag{4}$$

where $\phi(\cdot)$ denotes a Gaussian kernel function as

$$\phi(x, x_n; b) = \frac{1}{\sqrt{2\pi b}} e^{\frac{-(x-x_n)^2}{2b}}. \tag{5}$$

The parameter b determines the estimation accuracy of the PDF and is called bandwidth. The optimal b in (4) can be found by minimizing the mean integrated squared error (MISE) defined as

$$\begin{aligned} &\mathrm{MISE}\{\hat{f}\}(b) \\ &\quad = \mathbb{E}_f \int [\hat{f}(x) - f(x)]^2 dx \\ &\quad = \int \underbrace{(\mathbb{E}_f[\hat{f}(x)] - f(x))^2}_{\text{squared bias}} dx + \int \underbrace{\mathrm{Var}_f[\hat{f}(x)]}_{\text{variance component}} dx \end{aligned} \tag{6}$$

To simplify the solving procedure, the following (first-order) approximation MISE (AMISE) is instead used

$$\mathrm{AMISE}\{\hat{f}\}(b) = \frac{1}{4}b^2 \left\|f''\right\|^2 + \frac{1}{2N\sqrt{\pi b}} \tag{7}$$

where f'' denotes the second-order derivative of $f(x)$. By minimizing (7), the optimal b is solved as

$$b^* = \left(\frac{1}{2N\sqrt{\pi}\left\|f''\right\|^2}\right)^{2/5} \tag{8}$$

In (8), the $\left\|f''\right\|^2$ required to compute b^* can be estimated using the l-stage direct plug-in bandwidth selector (LsDPBS) method [24].

Existing RE detectors do not provide satisfactory performance when the SNR is low. This motivates us to propose a VSRE detector detailed in the next section.

III. THE VSRE-BASED NON-PARAMETRIC DETECTION METHOD

The block diagram of the proposed detector is shown in Fig. 1. From the figure, the observation sequence is input to a preprocessing module, which consists of a low-pass filter (LPF) block, a variable scale grouping (VSG) block, a fast Fourier transform (FFT) block and a KDE block. The LPF is applied such that the signal at an interested frequency band is extracted. The VSG block divides the entire sequence into multiple subsequences (groups) based on a given scale. In practical implementation, the number of groups, G_s, is chosen first then the corresponding scale S_{G_s} is determined as

$$S_{G_s} = \lfloor N/G_s \rfloor \tag{9}$$

where N is the length of the observation sequence and $\lfloor x \rfloor$ denotes the largest integer that is smaller than x. The G_s goes from 1 to $G = \lfloor T/T_{min} \rfloor$, where the T and $T_{\min}$ are the observation duration and the predefined minimum pulse width, respectively.

For a given scale S_{G_s}, the i-th subsequence is

$$\boldsymbol{x}_{G_s,i} = \begin{cases} \left[x_{(i-1)S_{G_s}+1}, \cdots, x_{iS_{G_s}}\right], & 1 \le i \le G_s - 1 \\ \left[x_{(G_s-1)S_{G_s}+1}, \cdots, x_N\right], & i = G_s \end{cases} \tag{10}$$

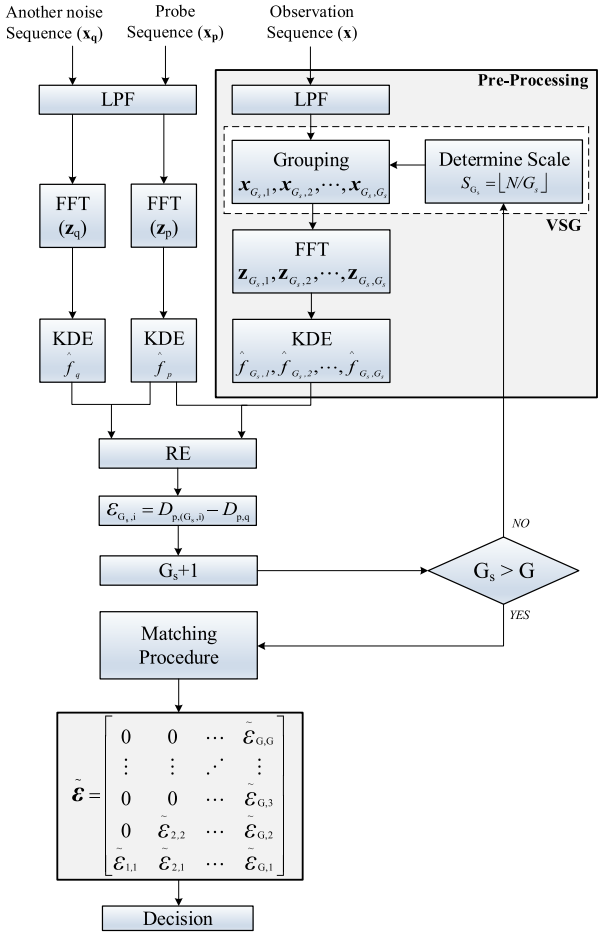

FIGURE 1. Block diagram of the VSRE detector.

It is noted the size of the last subsequence is $N - S_{G_s}(G_s - 1)$, which is not less than S_{G_s}.

Under low SNR scenarios, the pulse signals and ambient noise were indistinguishable in the time domain. In the frequency domain, however, a potential pulse tends to be more discernible [11]. Therefore, we choose to transform an observation subsequence into the frequency domain. The amplitude $z_{G_s,i}$ of FFT $\{\boldsymbol{x}_{G_s,i}\}$ is then sent to the aforementioned KDE for obtaining corresponding PDF estimation $\hat{f}_{G_s,i}(z)$. This completes the preprocessing. A similar procedure can be applied on $\boldsymbol{x}_p$ and $\boldsymbol{x}_q$ to obtain the PDF estimations $\hat{f}_p(z)$ and $\hat{f}_q(z)$. It is noted the two ambient noise sequences are not divided into subsequences and each is mapped to a single PDF. The RE between $\hat{f}_p(z)$ and $\hat{f}_q(z)$, $D_{p,q}$, can then be evaluated and used to determine the detection threshold.

The RE between $\hat{f}_p(z)$ and the PDF estimation $\hat{f}_{G_s,i}(z)$ of the i-th subsequence is also computed and denoted as $D_{p,(G_s,i)}$. Further, the RE difference, $\mathcal{E}_{G_s,i}$, for the i-th subsequence is

$$\mathcal{E}_{G_s,i} = D_{p,(G_s,i)} - D_{p,q} \tag{11}$$

Based on $\mathcal{E}_{G_s,i}$, a decision can be made according to (3). Such a decision, however, is risky. If the scale is much larger than the pulse width, the pulse may not be detected. On the contrary, if the scale is much smaller compared with the pulse duration, the pulse will occupy several subsequences and it is difficult to determine its start and end. To improve, we propose that a subsequence is declared to be a target pulse only when the following three conditions are also met: basically match (BM), slightly to the left (SL), and slightly to the right (SR), as will be shown shortly. To achieve that, we propose to perform a postprocessing for $\mathcal{E}_{G_s,i}$. If $\mathcal{E}_{G_s,i} > 0$ and $G_s \geqslant 3$, the frequency-domain subsequence $z_{G_s,i}$ and its neighbors $z_{G_s,i-1}$ and $z_{G_s,i+1}$ each will be divided into J blocks $\{z_{G_s,i}(j)\}_{j=1}^{J}$, $\{z_{G_s,i-1}(j)\}_{j=1}^{J}$ and $\{z_{G_s,i+1}(j)\}_{j=1}^{J}$. The corresponding RE differences are $\{\mathcal{E}_{G_s,i}(j)\}_{j=1}^{J}$, $\{\mathcal{E}_{G_s,i-1}(j)\}_{j=1}^{J}$ and $\{\mathcal{E}_{G_s,i+1}(j)\}_{j=1}^{J}$. After that, the postprocessing is performed: if any condition in the three cases of Table 1 is satisfied, $\tilde{\mathcal{E}}_{G_s,i} = \mathcal{E}_{G_s,i}$. Otherwise $\tilde{\mathcal{E}}_{G_s,i} = 0$. Last, if $\mathcal{E}_{G_s,i} \leq 0$, $\tilde{\mathcal{E}}_{G_s,i} = 0$.

Collecting postprocessed RE differences of all scales into a matrix leads to

$$\tilde{\boldsymbol{\mathcal{E}}} = \begin{bmatrix} 0 & 0 & \cdots & \tilde{\mathcal{E}}_{G,G} \\ \vdots & \vdots & \iddots & \vdots \\ 0 & 0 & \cdots & \tilde{\mathcal{E}}_{G,3} \\ 0 & \tilde{\mathcal{E}}_{2,2} & \cdots & \tilde{\mathcal{E}}_{G,2} \\ \tilde{\mathcal{E}}_{1,1} & \tilde{\mathcal{E}}_{2,1} & \cdots & \tilde{\mathcal{E}}_{G,1} \end{bmatrix} \tag{12}$$

Clearly, each column of $\tilde{\boldsymbol{\mathcal{E}}}$ corresponds to a particular scale.

With $\tilde{\boldsymbol{\mathcal{E}}}$, we are in the position to present the proposed VSRE pulse detection. We first map $\tilde{\boldsymbol{\mathcal{E}}}$ to a two-dimensional (2D) plane with G_s as abscissa and i as ordinate. The (1, 1) is set as the origin point. Based on the coordinates $\{(G_s, i)\}$ of all nonzero elements in $\tilde{\boldsymbol{\mathcal{E}}}$, slopes $\{\theta_{G_s,i} = \frac{i-1}{G_s-1}\}$ are calculated. Next, we divide the slopes, $\{\theta_{G_s,i}\}$, into groups, each containing close values thus corresponding to same pulse signal. It is easy to verify the larger the slope values, the later the pulse signal appears in the observation sequence. The coordinate of the maximum $\tilde{\mathcal{E}}_{G_s,i}$ within a given group is picked to determine the location of the pulse signal within the observation sequence. The detection procedure is finally summarized in Table 2.

TABLE 1. The conditions under which $\mathcal{E}_{G_s,i}$ is left unchanged.

►*Case 1*: $i = 1$
BM: $\{\mathcal{E}_{G_s,1}(j)\}_{j=1}^{J} > 0, \mathcal{E}_{G_s,2}(1) < 0$
SR: $\mathcal{E}_{G_s,1}(1) < 0, \{\mathcal{E}_{G_s,1}(j)\}_{j=2}^{J} > 0, \mathcal{E}_{G_s,2}(1) > 0,$ $\mathcal{E}_{G_s,2}(2) < 0$
►*Case 2*: $1 < i < G_s$
BM: $\mathcal{E}_{G_s,i-1}(1) < 0, \{\mathcal{E}_{G_s,i}(j)\}_{j=1}^{J} > 0, \mathcal{E}_{G_s,i+1}(1) < 0$
SR: $\mathcal{E}_{G_s,i}(1) < 0, \{\mathcal{E}_{G_s,i}(j)\}_{j=2}^{J} > 0, \mathcal{E}_{G_s,i+1}(1) > 0,$ $\mathcal{E}_{G_s,i+1}(2) < 0$
SL: $\mathcal{E}_{G_s,i-1}(J-1) < 0, \mathcal{E}_{G_s,i-1}(J) > 0, \{\mathcal{E}_{G_s,i}(j)\}_{j=1}^{J-1} > 0,$ $\mathcal{E}_{G_s,i}(J) < 0$
►*Case 3*: $i = G_s$
BM: $\mathcal{E}_{G_s,G_s-1}(J) < 0, \{\mathcal{E}_{G_s,G_s}(j)\}_{j=1}^{J} > 0$
SL: $\mathcal{E}_{G_s,G_s-1}(J-1) < 0, \mathcal{E}_{G_s,G_s-1}(J) > 0,$ $\{\mathcal{E}_{G_s,G_s}(j)\}_{j=1}^{J-1} > 0, \mathcal{E}_{G_s,G_s}(J) < 0$

TABLE 2. The procedure to find the pulse location in the VSRE detection.

Initialization

1. Get the coordinates and values of non-zero elements in $\tilde{\boldsymbol{\mathcal{E}}}$.
   Denote the row and column index sets as $\boldsymbol{R}$ and $\boldsymbol{C}$, the value set as $\boldsymbol{V}$.
2. Based on $\boldsymbol{R}$ and $\boldsymbol{C}$, a slope set $\boldsymbol{\theta}$ is obtained with $\boldsymbol{\theta}(k) = \frac{\boldsymbol{C}(k)-1}{\boldsymbol{R}(k)-1}$ $(k = 1, 2, ..., K)$, where K denotes the number of non-zero element
   Round $\boldsymbol{\theta}$ to the second decimal places.

Grouping

3. Combine any two values with a difference less than 0.01 to the smaller one in $\boldsymbol{\theta}$, leading to a new slope set $\tilde{\boldsymbol{\theta}}$. The size of $\tilde{\boldsymbol{\theta}}$, N_g, is the number of groups and its elements denote nominal slope values of the groups.
4. For l from 1 to N_g
   $m = 1$
   For k from 1 to K
   If $\left|\boldsymbol{\theta}(k) - \tilde{\boldsymbol{\theta}}(l)\right| \leqslant 0.01$
   $\boldsymbol{R}_l(m) = \boldsymbol{R}(k), \boldsymbol{C}_l(m) = \boldsymbol{C}(k), \boldsymbol{V}_l(m) = \boldsymbol{V}(k)$
   $m = m + 1$
   End
   End
   Based on $\boldsymbol{V}_l$, find the maximum in the l-th group and denote its index as m_l.
   End

Output

The number of detected pulses, N_g, and corresponding locations, $\left\{\frac{T}{\boldsymbol{R}_l(m_l)}(\boldsymbol{C}_l(m_l) - 1 : \boldsymbol{C}_l(m_l))\right\}_{l=1}^{N_g}$.

TABLE 3. The parameters of simulated signal pulses.

General Parameters		
Observation Duration (T)		8.72 s
Sampling Frequency (F_s)		20 KHz
Signal-to-Noise Ratio (SNR)		-5 dB
Cut-off Frequency of the LPF		6 KHz
Parameters of Combined Pulse Signal		
Pulse Type	LFM	CW
Pulse Width	80 ms	120 ms
Center Frequency	1200 Hz	1000 Hz
Bandwidth	50 Hz	0 Hz
Time Range	(2.53 : 2.61)s	(3.41 : 3.53)s

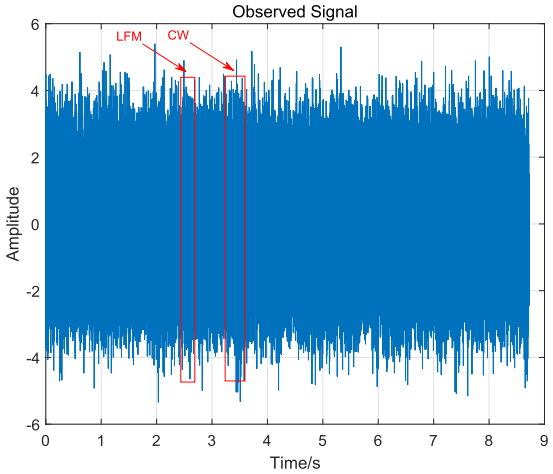

FIGURE 2. Demonstration of received signal which contains LFM and CW pulses.

IV. SIMULATION RESULTS

In this section, the proposed VSRE detector is evaluated by numerical simulations. We simulated the detection of a combined LFM and CW pulse signals, with the relevant parameters listed in Table 3. The bimodal noise model [25], [26] is adopted to simulate the ocean ambient noise.

On the receiver side, an observation sequence with a duration 8.72 s or equivalently $N = T \cdot F_s = 174400$ samples is recorded and shown in Fig. 2, where the locations of the LFM and CW pulses are marked. Both pulses are visually undistinguishable due to a low SNR.

In the VSRE detection, $T_{min} = 0.05$ s and the maximum number of subsequences $G = \lfloor T/T_{min} \rfloor = 174$. For the RE difference postprocessing, $J = 5$ is used. The mapping of the VSRE matrix, $\tilde{\boldsymbol{\mathcal{E}}}$, to the 2D plane is shown in Fig. 3. From the figure, there are 7 surviving points, which are divided into two groups. We can preliminarily determine that there exist two pulses in the observation sequence. According to the slope comparison, the first pulse (CW group) appears later than the second pulse in the observation sequence. Based on the comparison of corresponding scales, the first pulse has a larger width than the second one.

The coordinate of the point having the maximum RE difference is then found within each group for determining the pulse parameters. For the LFM group, the coordinate is (110, 33) based on which the pulse happens over the period

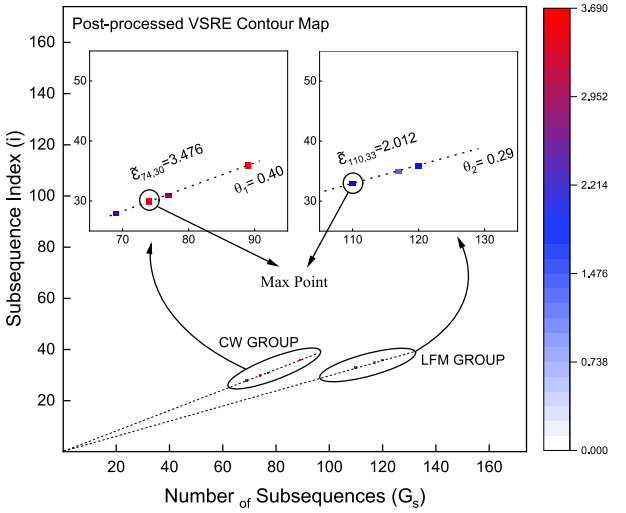

FIGURE 3. Demonstration of the postprocessed RE difference matrix.

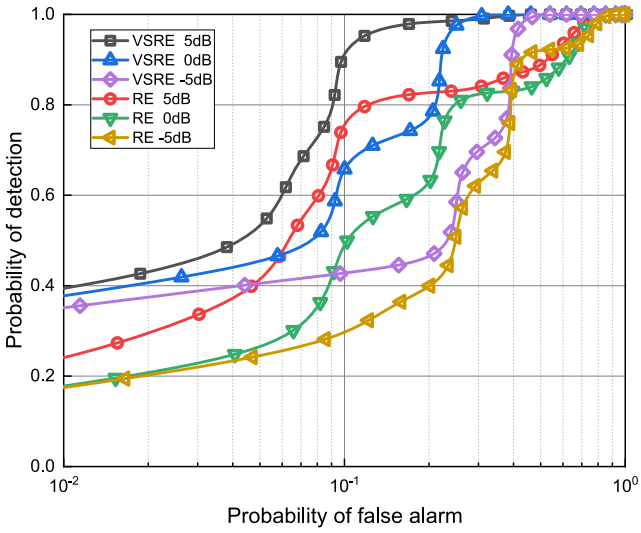

FIGURE 4. ROC comparison between a conventional RE detector and the proposed VSRE detector.

(2.537 : 2.616)s. For the CW group, the coordinate is (74, 30) leading to the pulse location of (3.417 : 3.535)s. The width estimations of the two pulses are then 79.27 ms and 117.84 ms, respectively. Clearly, the estimations are very close to actual values, demonstrating the high performance of the proposed VSRE detector.

Next, performance comparison between the conventional RE detector [16] and the proposed VSRE detector is made, in terms of the receiver operating characteristic (ROC). The comparison results are shown in Fig. 4, where it is obvious the VSRE detector outperforms the RE detector at different SNR levels.

V. EXPERIMENTAL RESULTS

The proposed VSRE detector was also tested by experimental data collected in an at-sea trial. The deployment of the at-sea trial is illustrated in Fig. 5, where the acoustic source and the receive hydrophone array are lowered 10 m and 30 m below

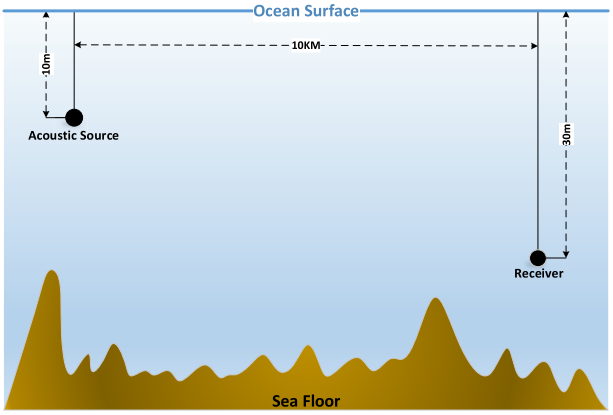

FIGURE 5. Illustration of the deployment of the at-sea trial.

TABLE 4. Parameters of transmitted combined pulse.

Pulse Number	Type	Pulse Width	Pulse Interval
At-sea trial data 1: CW+LFM			
Pulse I	CW	660.0 ms	0.32 s
Pulse II	LFM	140.0 ms	
At-sea trial data 2: LFM+CW			
Pulse I	LFM	360.0 ms	2.56 s
Pulse II	CW	630.0 ms	

the ocean surface, respectively. The horizontal transmission distance is about 10 km. Combined pulses were transmitted with their parameters listed in Table 4.

The data recording lasted for two hours on the receiver side at a sampling frequency of $F_s = 12.8$ KHz. In the off-line detection, we divide the data into packets of duration $T = 12$ seconds and detect the packets one by one individually. The length of each sequence is then $N = T \cdot F_s = 153600$, and the maximum number of groups $G = 120$ with a choice of $T_{min} = 0.1$ s. In the preprocessing, an LPF with a cut-off frequency of 6 KHz was used. No pulse signal was detected in the first 6 packets until the 7th one. In the following, the detection results for the 7th and 8th packets are discussed.

1) DETECTION RESULTS FOR PACKET 7

The postprocessed RE difference matrix is plotted in Fig. 6, where the surviving points are divided into two groups. For the group 1, the point with the maximum RE difference has a coordinate of $(18, 10)$, based on which the pulse location is determined as $(6.000 : 6.667)$ s. For the group 2, the point with the maximum RE difference has a coordinate of $(85, 50)$, leading to a pulse location of $(6.918 : 7.059)$ s. The widths of above detected pulse signals are then 666.67 ms and 141.18 ms, respectively.

In Fig. 7, the time-frequency graph (TFG) of the packet 7 is shown. It is obtained via the STFT method with its parameters determined from the detection results of the VSRE detector. From the figure, the group 1 denotes the CW pulse and group 2 denotes the LFM pulse.

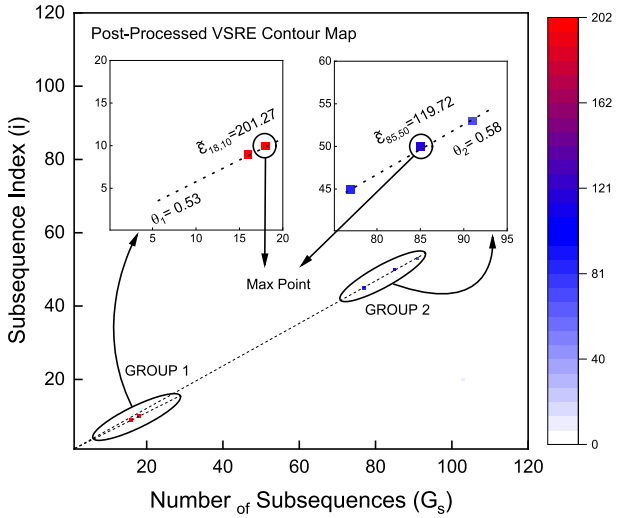

FIGURE 6. Demonstration of the postprocessed RE difference matrix (packet 7).

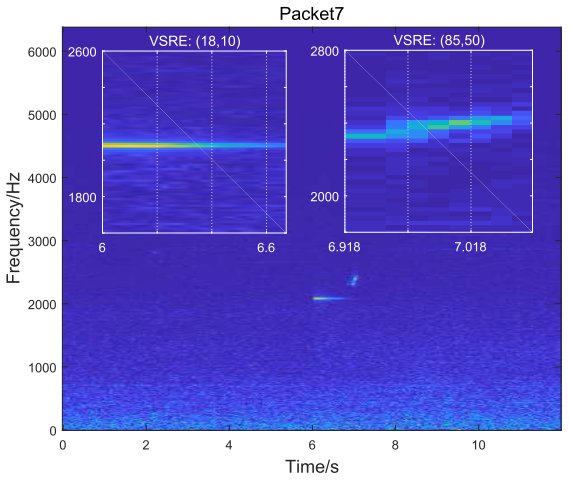

FIGURE 7. The STFT of packet 7, where the subgraphs represent the pulses detected at (18,10) and (85,50) by the VSRE detector.

2) DETECTION RESULTS FOR PACKET 8

The postprocessed RE difference matrix is plotted in Fig. 8, where the surviving points are divided into two groups. For the group 1, the point with the maximum RE difference has a coordinate of $(33, 19)$, based on which the pulse location is determined as $(6.545 : 6.909)$ s. For the group 2, the point with the maximum RE difference has a coordinate of $(19, 16)$, corresponding to the pulse location of $(9.474 : 10.105)$ s. The widths of above detected pulse signals are then estimated as 363.63 ms and 631.58 ms, respectively.

In Fig. 9, the TFG of the packet 8 is shown. It is again obtained via the STFT method with its parameters determined from the detection results by the VSRE detector. From the figure, the group 1 denotes the LFM pulse and group 2 denotes the CW pulse.

From above, the target pulses were successfully detected and their width estimations were very close to true values. This verifies the advantage of the proposed VSRE detector.

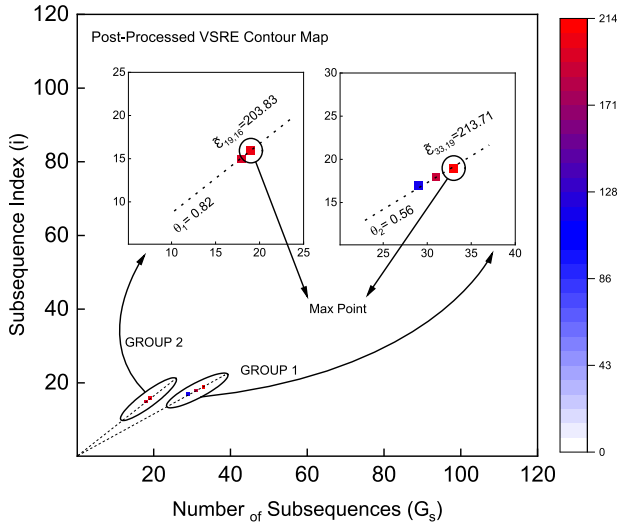

FIGURE 8. **Demonstration of the postprocessed RE difference matrix (packet 8).**

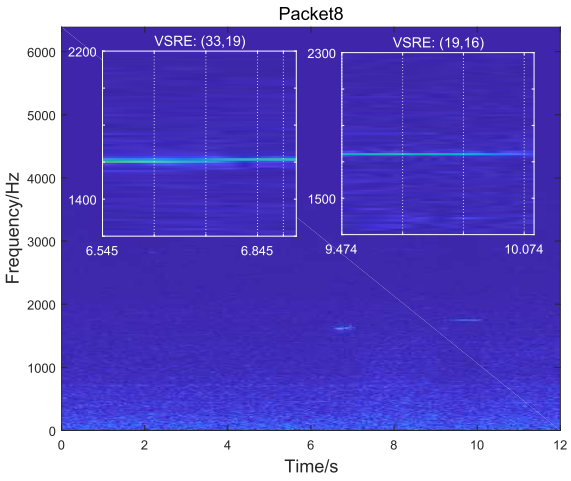

FIGURE 9. **The STFT of packet 8, where the subgraphs represent the pulses detected at (33,19) and (19,16) by the VSRE detector.**

VI. CONCLUSION

In this paper, an improved variable scale relative entropy (VSRE) detector was proposed for the detection of non-cooperative combined underwater acoustic pulse signals without prior information. It included a postprocessing procedure to improve the detection performance and also enable pulse parameters estimation. Simulation and at-sea experimental results were presented to verify the superiority of the enhanced VSRE detection scheme.

ACKNOWLEDGMENT

The authors would like to thank the anonymous reviewers and the editor Dr. E. Demirors for their careful reviews and valuable comments.

REFERENCES

[1] J. Marszal and R. Salamon, "Detection range of intercept sonar for CWFM signals," *Arch. Acoust.*, vol. 39, no. 2, pp. 215–230, Mar. 2015, doi: 10.2478/aoa-2014-0026.

[2] J. Marszal, "Experimental study of silent sonar," *Arch. Acoust.*, vol. 39, no. 1, pp. 103–115, Mar. 2015, doi: 10.2478/aoa-2014-0011.

[3] E. N. Sreedavy, R. Pradeepa, and V. P. Felix, "A novel algorithm for intercept sonar signal detector," in *Proc. Int. Symp. Ocean Electron. (SYMPOL)*, Cochin, India, Nov. 2009, pp. 3–8, doi: 10.1109/SYMPOL.2009.5664738.

[4] J. Hurka and D. Neumeister, "Entropy detection for intercept processing of sonar signals," Undersea Defence Technol., Rotterdam, The Netherlands, Tech. Rep., 2004.

[5] F. Hlawatsch and G. F. Boudreaux-Bartels, "Linear and quadratic time-frequency signal representations," *IEEE Signal Process. Mag.*, vol. 9, no. 2, pp. 21–67, Apr. 1992, doi: 10.1109/79.127284.

[6] P. M. David and B. Chapron, "Underwater acoustic signal analysis with wavelet process," *J. Acoust. Soc. Amer.*, vol. 87, no. 5, pp. 2118–2121, May 1990, doi: 10.1121/1.399179.

[7] B. Boashash and P. O'Shea, "A methodology for detection and classification of some underwater acoustic signals using time-frequency analysis techniques," *IEEE Trans. Acoust., Speech, Signal Process.*, vol. 38, no. 11, pp. 1829–1841, Nov. 1990, doi: 10.1109/29.103085.

[8] L. Qi, "Detection and parameter estimation of multicomponent LFM signal based on the fractional Fourier transform," *Sci. China F, Inf. Sci.*, vol. 47, no. 2, p. 184, 2004, doi: 10.1360/02yf0456.

[9] V. Kandia and Y. Stylianou, "Detection of sperm whale clicks based on the Teager–Kaiser energy operator," *Appl. Acoust.*, vol. 67, nos. 11–12, pp. 1144–1163, Nov. 2006, doi: 10.1016/j.apacoust.2006.05.007.

[10] Z. C. Zhang, Z. Jiang, H. Y. Wang, Z. G. Liu, and H. X. Jing, "Combination of time-reversal focusing and fractional Fourier transform for detection of underwater target in multipath environments," in *Proc. OCEANS Conf.*, Anchorage, AK, USA, 2017, pp. 1–5.

[11] K. M. Kumar, P. J. Sijomon, K. S. Joseph, D. M. Premod, V. S. Shenoi, and D. S. Bhai, "A novel intercept detection method for low-SNR targets using frequency domain processing," in *Proc. Ocean Electron. (SYMPOL)*, Kochi, India, Oct. 2013, pp. 23–30, doi: 10.1109/SYMPOL.2013.6701907.

[12] J. Luo, S. Wang, E. Zhang, and J. Luo, "Non-cooperative signal detection in alpha stable noise via Kolmogorov–Smirnov test," in *Proc. 8th Int. Congr. Image Signal Process. (CISP)*, Shenyang, China, Oct. 2015, pp. 1464–1468, doi: 10.1109/CISP.2015.7408114.

[13] J. Shu-Yao, Y. Fei, C. Ke-Yu, and C. En, "Application of stochastic resonance technology in underwater acoustic weak signal detection," in *Proc. OCEANS*, Shanghai, China, Apr. 2016, pp. 1–5, doi: 10.1109/OCEANSAP.2016.7485567.

[14] J. Tang, N. Li, Y. Wu, and Y. Peng, "On detection performance of MIMO radar: A relative entropy-based study," *IEEE Signal Process. Lett.*, vol. 16, no. 3, pp. 184–187, Mar. 2009, doi: 10.1109/LSP.2008.2011704.

[15] B. Tang, M. M. Naghsh, and J. Tang, "Relative entropy-based waveform design for MIMO radar detection in the presence of clutter and interference," *IEEE Trans. Signal Process.*, vol. 63, no. 14, pp. 3783–3796, Jul. 2015, doi: 10.1109/TSP.2015.2423257.

[16] P. C. Mignerey, A. Turgut, J. A. Schindall, and D. J. Goldstein, "Evaluation of relative entropy for distributed passive detection of weak acoustic signals," *IEEE J. Ocean. Eng.*, vol. 42, pp. 219–230, 2017, doi: 10.1109/JOE.2016.2546388.

[17] A. Downey, M. Sadoughi, S. Laflamme, and C. Hu, "Incipient damage detection for large area structures monitored with a network of soft elastomeric capacitors using relative entropy," *IEEE Sensors J.*, vol. 18, no. 21, pp. 8827–8834, Nov. 2018, doi: 10.1109/JSEN.2018.2868135.

[18] K. Ozcan, S. Velipasalar, and P. K. Varshney, "Autonomous fall detection with wearable cameras by using relative entropy distance measure," *IEEE Trans. Human-Mach. Syst.*, vol. 47, no. 1, pp. 31–39, Feb. 2017, doi: 10.1109/THMS.2016.2620904.

[19] K. Wei and S. L. Fang, "A novel search method of variable scale relative entropy for non-cooperative transient underwater acoustic pulse signals," in *Proc. Int. Cong. Expo. Noise Control Eng., Impact Noise Control Eng.*, Chicago, IL, USA, 2018, pp. 2130–2139.

[20] S. M. Kay, *Fundamentals of Statistical Signal Processing: Detection Theory*, vol. 2. Upper Saddle River, NJ, USA: Prentice-Hall, 1998.

[21] I. J. Good, "Maximum entropy for hypothesis formulation, especially for multidimensional contingency tables," *Ann. Math. Statist.*, vol. 34, no. 3, pp. 911–934, Sep. 1963, doi: 10.1214/aoms/1177704014.

[22] T. M. Cover and J. A. Thomas, *Elements of Information Theory*. Hoboken, NJ, USA: Wiley, 2006.

[23] S. Kullback, *Information Theory and Statistics*, Mineola, NY, USA: Dover, 1997.

[24] Z. I. Botev, J. F. Grotowski, and D. P. Kroese, "Kernel density estimation via diffusion," *Ann. Statist.*, vol. 38, no. 5, pp. 2916–2957, Oct. 2010, doi: 10.1214/10-AOS799.
[25] H. Amiri, H. Amindavar, and M. Kamarei, "Underwater noise modeling and direction-finding based on heteroscedastic time series," *EURASIP J. Adv. Signal Process.*, vol. 2007, no. 1, pp. 1–11, Dec. 2006, doi: 10.1155/2007/71528.
[26] F. Traverso, G. Vernazza, and A. Trucco, "Simulation of non-white and non-Gaussian underwater ambient noise," in *Proc. MTS/IEEE Oceans*, Yeosu, South Korea, May 2012, pp. 1–10, doi: 10.1109/OCEANS-Yeosu.2012.6263385.

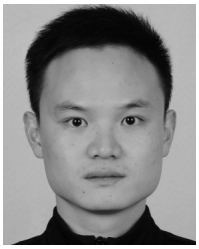

KUN WEI received the B.S. degree in electronic science and technology from the Changshu Institute of Technology, Changshu, China, in 2012, and the M.S. degree in signal and information processing from the Kunming University of Science and Technology, Kunming, China, in 2015. He is currently pursuing the Ph.D. degree with the Key Laboratory of Underwater Acoustic Signal Processing of Ministry of Education, Southeast University.

His research interests include underwater acoustic signal processing, detection, and parameter estimation.

SHILIANG FANG received the M.S. and Ph.D. degrees from Southeast University, Nanjing, China, in 1986 and 2009, respectively.

He is currently a Professor with the Key Laboratory of Underwater Acoustic Signal Processing of Ministry of Education, Southeast University. His research interests include signal processing, target detection and parameter estimation, and underwater target classification.

JUN TAO (Member, IEEE) received the B.S. and M.S. degrees in electrical engineering from the Department of Radio Engineering, Southeast University, Nanjing, China, in 2001 and 2004, respectively, and the Ph.D. degree in electrical engineering from the University of Missouri, Columbia, MO, USA, in 2010.

From 2004 to 2006, he was a System Design Engineer with Realsil Microelectronics, Inc. (a subsidiary of Realtek), Suzhou, China. From 2011 to 2015, he was a Senior System Engineer with Qualcomm, Inc., Boulder, CO, USA, working on the baseband algorithm and architecture design for the UMTS/LTE modem. Since April 2016, he has been with the School of Information Science and Engineering, Southeast University, as a Full Professor. His research interests include the general areas of wireless cellular communications, underwater acoustic communications, and localization and tracking, including channel modeling and estimation, turbo equalization, adaptive filtering, Bayesian inference, and machine learning.